Advances in Frontier Research on Engineering Structures
A. Cheshmehzangi and H. Bilgin (Eds.)

doi:10.3233/ATDE230185

Study on the Reasonable Clear Distance of Ultra-Shallow Buried Tunnel Group Through Expressway

Qiqi ZHENG[1], Chuanlin LI[2], Xinyu YAN[3]
CCCC Second Harbor Engineering Co. Ltd, Wuhan 430040, China

Abstract. Under the condition of super-shallow coverage and small spacing, the tunnel construction is easy to cause large structural deformation. The mechanical properties and supporting effect of tunnel with small spacing are summarized. Finite element software is used to simulate the effect on construction of tunnel group by changing the distance. The results show that with the increase of the distance, the settlement value of the middle tunnel has a smaller and smaller distribution law, when the distance exceeds 3m, the maximum main stress reduction changes less as the distance increases further, and the research results can provide a reference for the design and construction of similar tunnel group.

Keywords. Tunnel; Numerical Simulation; Surrounding Rock; Settlement

1. Introduction

In the construction of small clear distance tunnel group under the condition of ultra-shallow burial, the study of reasonable clear distance is always difficult. In the tunnel design, according to the different surrounding rock grades, the clear distance standard is generally between 1 and 5 times the tunnel diameter[1-3]. If the clear distance is greater than this range, the interaction between the double tunnels is considered to be negligible. Under the premise of stable surrounding rock, the clear distance can be reduced to how small, and no unified conclusion has been formed[4-8]. Based on the construction of ultra-shallow buried tunnel group of Yangang-East interchange project in Shenzhen, the displacement and stress development rules of the tunnel are analyzed, through comprehensive comparative analysis, the reasonable clear distance of the tunnel under the expressway is obtained.

[1] Qiqi ZHENG, CCCC Second Harbor Engineering Co. Ltd, Wuhan 430040, China; e-mail: 379014435@qq.com
[2] Chuanlin LI, CCCC Second Harbor Engineering Co. Ltd, Wuhan 430040, China; e-mail: xinyuwithyou@126.com
[3] Corresponding Author: Xinyu YAN, CCCC Second Harbor Engineering Co. Ltd, Wuhan 430040, China; e-mail: 347832087@qq.com

2. Engineering Situation

In the Yangang-East interchange tunnel group, the ramp LY, C and E crosses the Yan-Ba highway , and the angle between the tunnel and the highway is about 43°. The minimum buried depth of the tunnel is 1.6m~4.6m, the upper layer is clay and stone, and the lower layer is strongly weathered granite, which is constructed by the new Austrian method. Due to the poor geological conditions, the excavation of the tunnel group is easy to produce large deformation, so the measures such as advance reinforcement and support reinforcement should be taken. The project plan is shown in Figure 1, the structure of the tunnel group in Figure 2.

Figure 1. overall planning of tunnel group

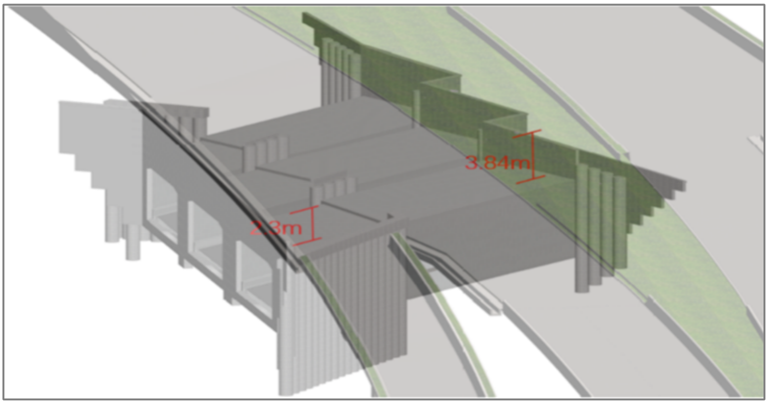

Figure 2. structural cross-sectional map

3. Finite Element Model

3.1. Model Foundation

The underpass tunnel group is a three-hole structure with an excavation span of 11.7m,12.2m,12.7m, an excavation height of 8.65m and an initial support thickness of

35cm. The E and C channels on both sides are constructed first, and then the LY channels. The FLAC 3D is used to simulate the construction control effect of the tunnel group. According to the Saint Venan principle, the left and right sides of the finite element model are 5 times the tunnel width, and the elastoplastic model and the mohr-coulomb criterion are used[9-11]. Constrained horizontal displacement around the model, constrained vertical displacement at the bottom and a free boundary at the top. The computational models are shown in Figure 3.

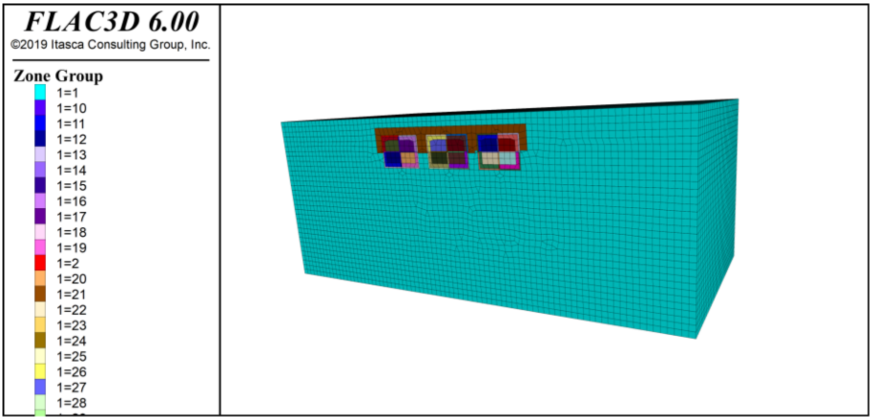

Figure 3. Grid computing model

3.2. Parameters of geo-material

The main geological parameters of the tunnel crossing are shown in Table 1.

Table 1. Physical and mechanical parameters of geo-material

formation	modulus of elasticity /GPa	cohesion C/kPa	Internal friction angleψ/°	unit weight γ/kn/m^3	Poisson ratio
clay	0.00285	8	12	18.5	0.45
fully weathered granite	0.00525	27	22.2	18.8	0.43
strong weathering granite	1.25	60	22.8	20.0	0.29
medium weathered granite	5	500	35	25.0	0.25
C25 class concrete	25	--	--	23	0.2

3.3. Monitoring Measurement Point

L1~L3 is selected as subsidence observation point of channel E, M1~M3 as the subsidence observation point of channel LY,R1~R3 as the subsidence observation point of channel C. L4~L6 as the uplift point of E channel, M4~M6 as the uplift point of LY channel, R4~R6 as the uplift point of C channel,L7~L8 as the uplift point of channel E, M7~M8 as the uplift point of channel LY, and R7~R8 as the horizontal deformation measuring point of channel C . H1~H9 as the subsidence point of road surface, as shown in Figure 4.

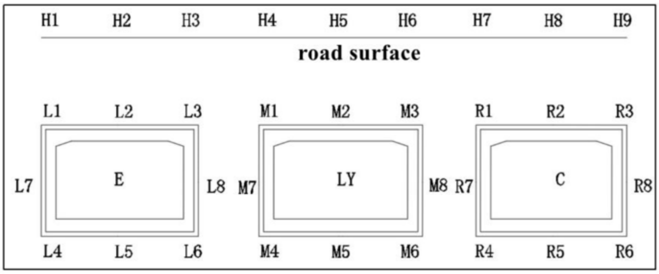

Figure 4. Distribution map of monitoring points

4. Analysis of Computational Results

4.1. Analysis of Deformation of Surrounding Rock

(1) the designed clear distance is 1.5 m

With middle LY tunnel as the main analysis object, vertical and horizontal deformation rules as shown in figure 5 (a) and figure 6 (a), the results show that at the position of the arch, the vertical deformation drops first, then rises, then drops, and finally tends to stabilize. The maximum vertical deformation of M1, M2 and M3 is 7.55mm, 8.25mm, 7.84mm, respectively. The maximum horizontal deformation of M7 and M8 is 4.98mm,-5.96mm.

(2) the designed clear distance is 3 m

With middle LY tunnel as the main analysis object, vertical and horizontal deformation rules as shown in figure 5 (b) and figure 6 (b), the results show that at the position of the arch, the vertical deformation drops first, then rises, then drops, and finally tends to stabilize. The maximum vertical deformation of M1, M2 and M3 is 6.50mm, 7.07mm, 6.76mm, respectively. The maximum horizontal deformation of M7 and M8 is 3.30mm, -4.07mm.

(3) the designed clear distance is 6 m

With middle LY tunnel as the main analysis object, vertical and horizontal deformation rules as shown in figure 5 (c) and figure 6 (c), the results show that at the position of the arch, the vertical deformation drops first, then rises, then drops, and finally tends to stabilize. The maximum vertical deformation of M1, M2 and M3 is 5.91mm, 6.12mm, 5.98mm, respectively. The maximum horizontal deformation of M7 and M8 is 2.89mm, -3.61mm.

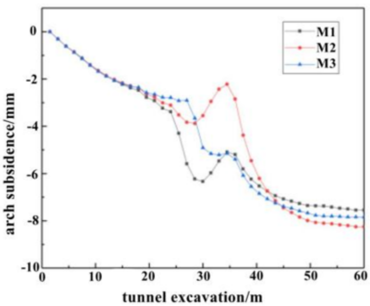

(a)

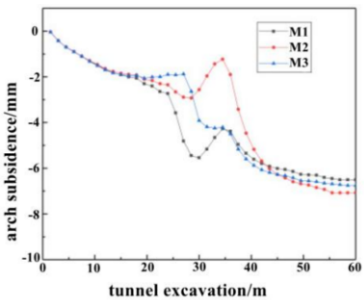

(b)

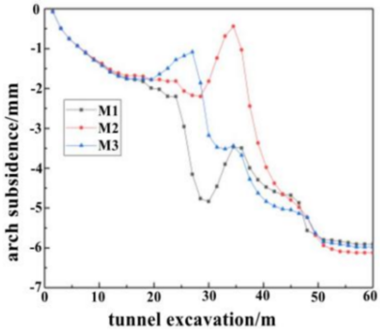

(c)

Figure 5 Vertical deformation curve

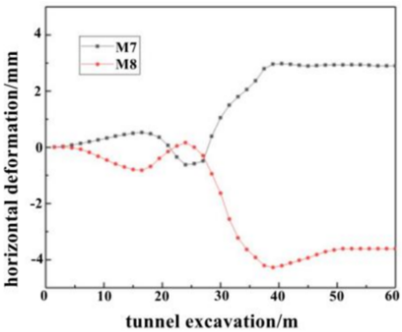

(a)

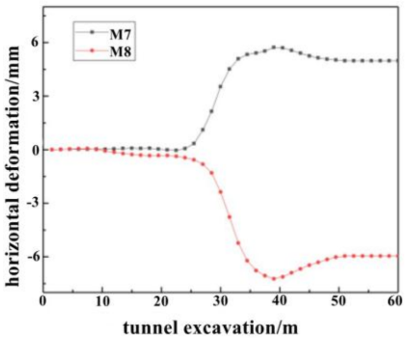

(b)

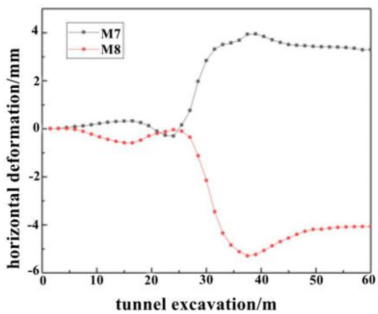

(c)

Figure 6. Horizontal deformation curve

The results show that with the increase of clear distance, the vertical deformation of tunnel arch is M-type distribution. As the clear distance of the tunnel increases, the settlement value of the middle tunnel becomes smaller and smaller.

4.2. Structural Stress

The maximum main stress of the surrounding rock under different clear distances is shown in Figure 7 to Figure 9. The results show that the maximum main stress of the tunnel is located on the intermediate pillar of channels E and C. With the increase of the clear distance, the maximum main stress of the surrounding rock gradually decreases. When the clear distance changes from 1.5m to 3m, the maximum stress of the surrounding rock decreases greatly, the maximum stress between E and LY decreases from 1.28MPa to 0.76MPa, and the maximum stress between C and LY decreases from 1.27MPa to 0.86MPa. When the appropriate excavation scheme is adopted and the middle rock mass is strengthened, the clear distance between the tunnels can be continuously reduced.

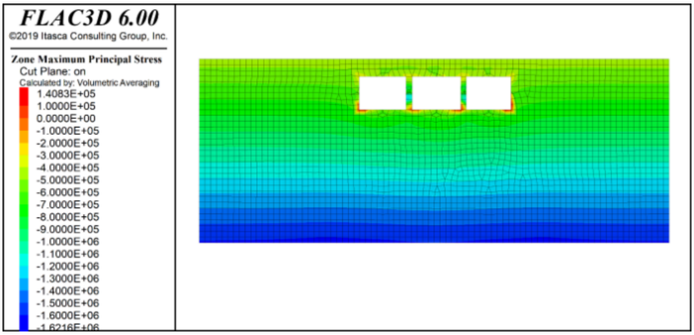

Figure 7. Main stress cloud map with a clear distance of 1.5m

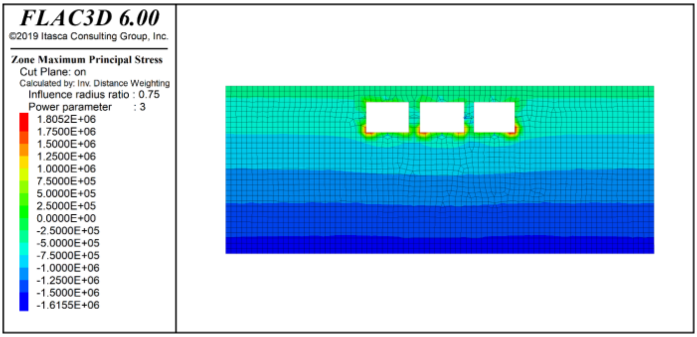

Figure 8. Main stress cloud map with a clear distance of 3m

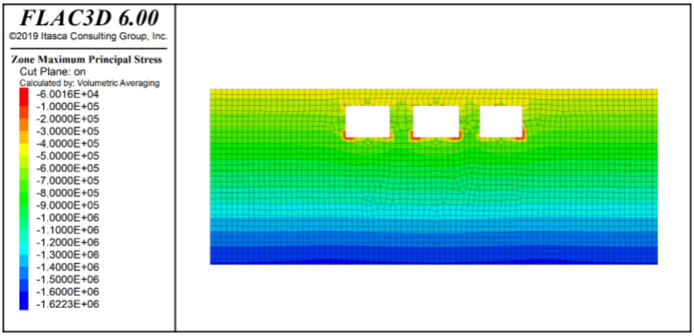

Figure 9. Main stress cloud map with a clear distance of 6m

5. Conclusion

The deformation and stress change of tunnel group under different clear distances brings up the following conclusions:

(1) With the increase of the clear distance, the vault settlement cross section of the tunnel is M-shaped distribution. However, with the increase of the clear distance, the settlement performance of the middle tunnel becomes smaller and smaller.

(2) With the increase of the clear distance, the maximum main stress of the surrounding rock gradually decreases. When the clear distance exceeds 3m, the decrease of the maximum main stress decreases less, with the further increase of the clear distance.

(3) The reasonable clear distance is relative, not only to ensure the safety and quality of the project, but also to meet the requirements of established planning, design, construction and investment conditions. In the case of tunnel group under the road, the clear distance should not be less than 3m.

(4) Due to the simplification of the model, some load parameters in the calculation process may be different from the actual situation, the results are only used as reference, and the actual deformation is mainly monitored by site construction.

References

[1] Zeng Runzhong, Zhan Tao.parameters for pipe roof support of shallow bored tunnels[J].Modern Tunnelling Technology, 2018, 55（1）:211-215(in Chinese)

[2] He Xiaolong. design and construction of a shallow buried subway undercrosss a large box culvert[J]. Soil Engineering and Foundation, 2014, 28（1）:22-25(in Chinese)

[3] Li Jianlin, Wu Jingang. study on the design and construction method for the large-span highway tunnel with small interval[J]. Modern Tunnelling Technology, 2019, 56(05):157-162(in Chinese)

[4] Tang Yuchun, Xu Llinsheng. comments on construction of closely-spaced tunnels[J]. Tunnel Construction, 2007(01):22-25(in Chinese)

[5] Li Zhiqing, Ding Chunlin. space-time effect of surrounding rock deformation in shallow-depth large section loess tunnels[J]. Journal of East China Jiaotong University, 2014, 31（4）:6-10(in Chinese)

[6] Shi Zuojing. research on application of surface grouting in super-shallow embedded tunnels[J]. Technology of Highway and Transport, 2016, 32（3）:103-111(in Chinese)

[7] Dai Shimin. simulation analysis of soil pre-reinforcement for large-section shallow buried covered excavation tunnel in soft soil[J]. Construction Technology, 2020, 49（19）:87-90(in Chinese)

[8] Zhang Xuefeng, Wang Yanbing. risk analysis and countermeasures for shallow tunnels with small clear distance crossing beneath railways[J]. Journal of Shijiazhuang Tiedao University（Social Science）, 2015, 28（3）:49-55(in Chinese)

[9] Sadeghiyeh S M, Hashemi M, Ajalloeian R. Comparison of permeability and groutability of Ostur Dam site rock mass for grout curtain design[J]. Rock Mechanics and Rock Engineering, 2013, 46(2):341-357.

[10] Turkmen S. Treatment of the seepage problems at the Kalecik Dam (Turkey)[J]. Engineering Geology, 2003, 68(3):159-169.

[11] Davis G M, Horswill P. Groundwater control and stability in an excavation in Magnesian Limestone near Sunderland, NE England[J]. Engineering Geology, 2002, 66(1):1-18.